Effects of an extreme flood event on an alpine karst system

Contents lists available at ScienceDirect

Journal of Hydrology

journal homepage: http://ees.elsevier.com

Research papers

Effects of an extreme flood event on an alpine karst system

Alessia Nannoni [a,1,*], Bartolomeo Vigna [b], Adriano Fiorucci [b], Marco Antonellini [a], Jo De Waele [a]

[a] Department of Biological, Geological and Environmental Sciences, University of Bologna, Via Zamboni 67, 40126 Bologna, Italy
[b] Department of Environment, Land and Infrastructure Engineering (DIATI), Polytechnic of Turin, Corso Duca degli Abruzzi 24, 10129 Torino, Italy

ARTICLE INFO

This manuscript was handled by Huaming Guo, Editor-in-Chief

Keywords
Alpine karst
Extreme flood event
Discrete monitoring
Hydrochemistry
Unsaturated zone
Structural setting

ABSTRACT

The effects of an extreme storm (501 mm of rainfall in less than five days) were monitored in an alpine show cave to assess the characteristics of its aquifer unsaturated and saturated zones. The selected cave, *Bossea* (SW Piedmont, Italy), is an excellent test site for hydrological investigation of karst systems, because it hosts an underground karst laboratory since the late 70 s. The investigation was carried out by means of an integrated approach that combined measurements of flow discharge, physico-chemical parameters, major chemical components, and trace elements (metals, Rb, Ba, Sr and REE). The hydrology and hydrochemistry of the main underground river and two of its secondary tributaries (a drip site and a small secondary inflow) draining the unsaturated zone were monitored during the November 2016 flood, an exceptional hydrological event (estimated recurrence time of 200 years) that caused severe damages in the whole southwestern Piedmont region. The results of the 2016 monitoring were compared with those of another less extreme flood occurred in 2011 (recurrence time of 20 years). The karst system showed an impulsive response to flooding at the catchment and at the individual inflow scales, but each site exhibited a characteristic response due to the complex geological and structural setting of the cave system. The development of this karst system is, in fact, related to the lateral and vertical juxtaposition of rocks with different lithologies and mechanical properties, which form different hydrogeologic compartments. Coupling hydrograph, chemograph analysis and REE normalized patterns permitted to assess which compartments were activated during each phase of the floods. In particular, it was possible to recognize a progressive increasing contribution of the non-carbonate lithologies to flow during the peak of the flood for both the two unsaturated inflows and the main underground river, suggesting the activation of larger portions of the aquifer. However, the response of each individual unsaturated inflow is more influenced by its recharge system architecture rather than the magnitude of the meteorological event. Similar complex geological and lithological karst systems are typical of many areas characterized by orogenetic processes (Alps, Rocky Mountains, Caledonides, etc.), but despite them being relatively widespread, the hydrodynamics of these aquifers is still poorly understood. This study affirms that only long-term and well-integrated monitoring and sampling can help unravel the behavior of such complex karst systems.

1. Introduction

Understanding flow dynamics in karst systems has many implications on water quality assessment and storage estimation. Karst aquifers are vulnerable to contamination and it is fundamental to assess how contaminants are transmitted from the surface to the karst springs (Hartmann et al., 2014; Mudarra and Andreo, 2011; Perrin et al., 2003). In this perspective, the unsaturated zone plays a pivotal role, because it regulates the transmission of water, chemicals, and sediments to the saturated zone below. Monitoring unsaturated inflows (drip sites) is useful to infer the flow dynamics and structure of the unsaturated zone whereas large karst springs are representative of relatively bigger portions of the aquifer (Baedke and Krothe, 2001; Grasso and Jeannin, 2002; Poulain et al., 2018, 2015; Pronk et al., 2008). Even more important is the interplay between temporal and spatial variability of the hydrodynamic response of the aquifer to rainfall/infiltration events. Both are strictly related to the architecture of the catchment and secondarily to the meteorological conditions (Jex et al., 2012; Markowska et al., 2015).

The intrinsic heterogeneity of karst flow is further complicated in structurally complex systems where the architecture of the aquifer is strongly controlled by tectonics, fractures, and/or drainage networks developed in different lithologies. Among geologically-complex karst systems, those that developed in an orogenic context, such as the Alpine chain, are widely recognized as important water resources (Plan et al., 2009). Uplift and deepening of the base level due to deglacia-

* Corresponding author.
E-mail address: alessia.nannoni2@unibo.it (A. Nannoni)
[1] Present address: Department of Earth Sciences, University of Florence, Via La Pira 4, 50121 Firenze, Italy.

https://doi.org/10.1016/j.jhydrol.2020.125493
Received 13 March 2020; Received in revised form 27 August 2020; Accepted 29 August 2020
Available online xxx

tion strongly affected the development of this kind of karst (Audra et al., 2007). In fact, alpine karsts are characterized by mid- to high-altitude recharge areas, whereas discharge is commonly located at the valley bottom. This arrangement caused the development of extensive unsaturated zones (Vigna and Banzato, 2015). The orogenetic process led also to the complex juxtaposition of carbonate and non-carbonate lithologies. Recharge, therefore, is not limited to karstified rocks, and the allogenic component can be relevant. In such systems, the use of multiple hydrochemical indicators is recommended to understand the contribution to flow from different compartments of the aquifer. For this purpose, it is useful to couple major ions, trace elements, and Rare Earth Elements (REE) analyses together with chemograph interpretation (Berglund et al., 2019; De la Torre et al., 2020; Filippini et al., 2018; Gill et al., 2018; Möller et al., 2006).

Previous studies helped to improve conceptual models of karst aquifers but, as pointed out by Berglund et al. (2019), critical knowledge gaps persist regarding flow paths and recharge processes. This lack of knowledge is even more pronounced where dealing with exceptional conditions such as extreme flood events or persistent droughts with long recurrence intervals. Previous studies dealt with either karst springs (Desmarais and Rojstaczer, 2002; Doctor et al., 2006; Vesper and White, 2004), or drip site (Baldini et al., 2012; Liu et al., 2014) responses to precipitation events of various magnitudes but an integrated approach that involves the investigation of both springs and unsaturated inflows is not common.

1.1. Objectives

This study reports the results of the hydrological and hydrochemical response of an alpine karst system to an extreme flood event occurred in November 2016 in Southern Piedmont (Italy), which has an estimated recurrence time of more than 200 years (ARPA Piemonte and Regione Piemonte, 2018). The main underground river and two unsaturated inflows are presented here; the flood following another storm event in November 2011 and with similar hydrological conditions (end of baseflow phase – onset of autumnal recharge) but with a significant lower magnitude (estimated recurrence time of about 20 years) is also reported for comparison. This is the first attempt to monitor a flood event in an Italian cave (*Bossea* show cave) where water flow is controlled by the local structural setting (Antonellini et al., 2019). The main objective of this study is to assess the effect of extreme meteorological conditions on the hydrodynamic response of a structurally complex karst aquifer and, in particular, to recognize the different contributions of distinct hydrogeological compartments of the catchment to unsaturated flow and to the underground river. This objective is accomplished by means of detailed chemograph analysis and discrete hydrochemical sampling. The *Bossea* cave is an excellent test site to study karst hydrology, because it hosts an underground scientific laboratory that monitors groundwater hydrology and hydrochemistry since the late 70 s (Vigna et al., 2017b), so that a large database on unsaturated inflows and main underground stream hydrodynamic behavior is available for comparison with the data gathered during the 2016 and 2011 extreme flood events. Moreover, the understanding of the mechanisms that control flood development is important for risk evaluation in a show cave that attracts more than 30,000 visitors every year.

2. Study area and description of the meteorological events

2.1. Bossea karst system

The *Bossea* karst system is in the Ligurian Alps (Southern Piedmont, Italy; Fig. 1a), with a colluvium-covered mid-altitude karst catchment of about 5.5 km^2, comprised between 800 and 1700 m asl draining water from the *Corsaglia* and *Maudagna* valleys (Civita and Vigna, 1985; Peano et al., 2005; Vigna and Doleatto, 2008). The surface is characterized by steep SE-facing slopes with bare rock outcrops and a thin soil cover. The recharge area comprises losing streams (*Rio Bertino* and *Rio Roccia Bianca* brooks, Fig. 1b) with variable flowrates.

The present-day architecture of the *Bossea* karst system is controlled by the Alpine tectonics: subvertical faults (e.g. the *Borello*, *Fontane*, and *Prel* lines, Fig. 1b) form rock compartments where the metamorphosed folded Mesozoic carbonate blocks are in lateral and vertical contact with the underlying volcanoclastic (Permian) and clastic rocks (Lower Triassic) (Fig. 1b). The compartments are made up mostly of marbles (*High-hydraulic conductivity complex, H-Kc*) and secondarily of quartzite, shales and metavolcanics, the latter acting as aquitards or forming small perched aquifers (*Low-hydraulic conductivity complex, L-Kc*). Hence, the recharge is partly diffuse and partly from allogenic streams that release water into the fractured portions of the *L-Kc* (Banzato et al., 2011; Vigna et al., 2017).

The *Bossea* show cave developed along a detachment surface between the isoclinally folded sequence made up of marble, quartzite, and shale and the underlying metavolcanic sequence (Fig. 1c, d; Antonellini et al., 2019). The main underground stream, the *Mora* river (TM), flows along this major detachment in the downstream part of the show cave. The *Mora* river is fed by several secondary tributaries that drain water from the unsaturated zone that developed in the *H-Kc*. The water resurfaces along the *Corsaglia* river (812 m asl) from a set of karstified bedding junctions. The cave entrance (836 m asl) is a semi-active conduit that discharges water during strong infiltration events, when the springs along the *Corsaglia* river cannot convey the entire water flow. More information about the geology of the area and *Bossea* cave speleogenesis can be found in Antonellini et al. (2019).

2.2. The November 2016 flood event and previous floods

On 21st-25th November 2016, the western and southern Piedmont were affected by strong precipitations. Heavy rainfall struck the southern Piedmont first (November 22nd-23rd) and then reached the western sectors of the Italian region. The strongest rainfall intensity was recorded between November 24th and November 25th (26.8 mm/h) near the *Bossea* cave. The highest cumulative precipitation (632.6 mm) was recorded in the uppermost section of the *Tanaro* valley (*Corsaglia* river being one of *Tanaro* river tributaries) and represents more than 50% of the average annual rainfall. This meteorological event caused floods in the whole Southern Piedmont, the strongest floods occurred in the *Tanaro* river and its tributaries with a magnitude that has an estimated 200 years recurrence time (ARPA Piemonte and Regione Piemonte, 2018). This event caused one of the strongest flood events on record in the *Bossea* cave with a maximum discharge of 1960 l/s. Total amounts of rainfall were similar during the November 2011 and 2016 storms (Table 1). However, the 2011 precipitation event lasted longer. Moreover, the daily rainfall amount and the maximum hourly rainfall (17.4 mm/h, ARPA Piemonte, 2011) were significantly lower than the values observed during the 2016 storm (Table 2).

3. Materials and methods

The main underground river (*Mora* river, TM; Fig. 1c, 1d) was equipped with an STS (Opera, Milano, Italy) integrated sensor and data logger for water level (L), temperature (T), and electrical conductivity (EC). Three water samples were collected for hydrochemical analyses before, during, and after the November 2011 storm event. An automatic water sampler (ISCO model 2900 sampler, ISCO Inc., Lincoln, USA) with a six hours sampling frequency was installed during the 2016 flood event for hydrochemical monitoring; the sampling started on the 20th of November (12:00 AM) and ended on the 2nd of December at 6:00 AM (the flood peak happened on the 24th of November 11:00 PM).

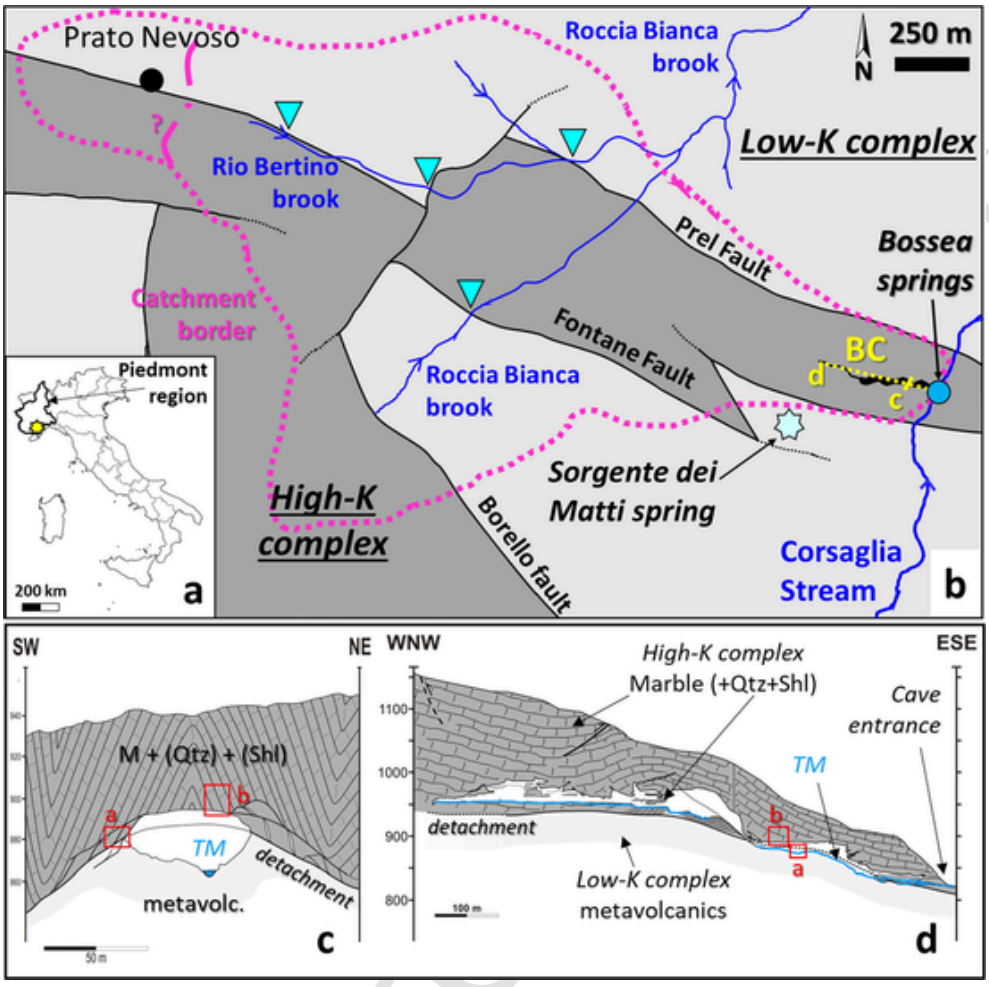

Fig. 1. (a) Index map with study site (yellow dot). (b) Simplified geological map of the *Bossea* cave (labelled BC) and cross-sections location (dotted yellow lines); sinkholes are represented by cyan triangles. (c) Simplified SW-NE oriented geological cross-section (M, Qtz and Shl stand respectively for marble, quartzite and shale); the red rectangles mark the position of the monitored unsaturated inflows ("a" stands for *Polletta* inflow and "b" stands for *Milano* drip site; see Section 5.4). (d) WNW – ESE oriented cross-section, TM represent *Mora* river. Modified after Antonellini et al. (2019).

Table 1
Overview of the major precipitation events occurred in the *Corsaglia* valley recorded by the *Borello* meteorological station (1.5 km S of *Bossea* cave).

Corsaglia valley major precipitation events						
	1994/11	1996/10	1997/11	2011/11	2016/11	
duration (days)	4	2	2	6	5	
total rainfall (mm)	0.0	208.2	190.0	424.4	501.0	
max daily rainfall (mm)	166.8	122.6	160.6	118.8	246.4	
			Storm 2011/11 daily rainfall			
day	03/11/2011	04/11/2011	05/11/2011	06/11/2011	07/11/2011	08/11/2011
mm	33.20	98.60	118.80	101.20	21.40	51.20
			Flood 2016/11 daily rainfall			
day	21/11/2016	22/11/2016	23/11/2016	24/11/2016	25/11/2016	
mm	109.6	38.0	79.8	246.4	27.2	
	2011	2016				
total yearly rainfall (mm)	1279.8	1587.2				
total november rainfall (mm)	437.0	551.8				
Mean total rainfall per year (mm)	1409.5					

Several *Mora* river secondary tributaries (or inflows), equipped with concrete weirs and an STS integrated sensor and data loggers for water level (L), temperature (T), and electrical conductivity (EC), were monitored during the two storms; the loggers recorded 1 to 4 measurements per hour. The secondary tributaries presented in this paper represent ideal examples of structural control on flow in the *Bossea* karst. The

Table 2
Statistical summary of *Mora* river hydrological and physico-chemical monitoring during the 2011 and 2016 floods. Mean values of each parameter are reported for comparison.

		Q*	T**	EC**
		l/s	°C	µS/cm
mean				
	Mean	177.9	7.53	219.6
	Median	124.7	7.55	218.0
	Min	33.8	6.74	196.0
	Max	1960.2	7.92	265.0
2011				
	Mean	263.8	7.62	220.8
	Range	1541.7	0.40	22.0
	Min	66.6	7.45	214.0
	Max (Flood peak)	1608.3	7.85	236.0
2016				
	Mean	280.9	7.5	225.2
	Range	1877.4	0.3	23.0
	Min	82.9	7.4	217.0
	Max (Flood peak)	1960.2	7.7	240.0
	time intervals for mean	*	1982–2019	
	values calculations	**	2008–2019	

Polletta (PTTA, rectangle "a" in Fig. 1c, d) is a small spring inflow that discharges water along the detachment between the Mesozoic carbonate sequence and the underlying Permian metavolcanics. The *Milano* (M) drip site discharges along a subvertical bedding surface in the marbles (rectangle "b" in Fig. 1c, d).

Water samples of both inflows were collected for hydrochemical analysis before, during, and after the 2011 storm and the 2016 flood events. Two water samples were collected for each inflow, one was taken in a 500-ml bottle for major ion content, the other one was acidified in situ with HNO_3 (65%) and kept in a 100-ml bottle for metals and lanthanides contents. Sample temperature, pH and EC were measured in situ. The samples collected by the automatic sampler used 500-ml bottles; 100 ml water was taken from each bottle and acidified with the same procedure and purpose explained above. The first 24 samples were taken from the automatic sampler after six days of sampling and the following 24 samples were collected at the end of the monitoring.

Water analysis was done at the DIATI laboratory, Polytechnic of Turin (Italy). The determination of Ca^{2+}, Mg^{2+} was carried out by means of ion-selective electrode, HCO_3^- was determined by acid-base titration with instrumental control of pH. Anion concentrations were determined by ion chromatography (Metrohm 881bIC Pro). Na^+ and K^+ were determined by Atomic Absorption Spectroscopy (AAS); NH_4^+ was analyzed by UV–VIS spectrophotometry. An X Series 2 ICP-MS (Thermo Scientific) was employed for trace elements determination (metals and lanthanides). The detection limit (LOD) for ion chromatography and titration was 0.1 mg/l, whereas it was 0.05 mg/l for AAS. The detection limit was 0,1 ppb for metals and 1 ppt for the lanthanides. REE values below the LOD were counted in the total REE amount calculation and for normalization (see below). The lanthanide concentrations were normalized to the *Post Archean Australian Shale* (PAAS, McLennan, 1989). The purpose of the normalization was to infer the type of rocks drained during the flood (Berglund et al., 2019; Gill et al., 2018). The hydrochemical composition of a nearby spring was taken as reference of the non-carbonate water drained from the *L-Kc* (*Sorgente dei Matti* spring, SdM).

Rainfall and air temperature data were collected at the *Borello* meteorological station of the Piedmont Regional ARPA Agency. This station is located at 1.5 km from the cave at an altitude of 1005 m asl, and is equipped with a rain gauge PMB2/R – CAE. Air temperature was used as a proxy for rainfall temperature.

4. Results

4.1. Mora river 2011 and 2016 monitoring

The 2011 storm event started on the 3rd of November and ended five days later, with most rainfall on November 5th. The underground *Mora* river (Fig. 2) reached its peak flow on the morning of November 6th, 37 h after the peak in hourly precipitation (17.4 mm on November 4th 07:00 PM). After the peak flow, the recession limb was perturbed by additional precipitation (November 8th-9th) and normal flow values returned in 8 days. Water temperature decreased (0.4 °C of variation) when water flow began to rise. After the peak flow, T rose continuously and did not return to pre-storm values for more than 3 months. EC increased intermittently during the rising limb of flow and reached its maximum (236.0 µS/cm) on November 13th, returning to pre-storm values (218.0 µS/cm) in 2 weeks. The alkali to chloride ratio remained close to 1 in all samples (see Fig. 2). Total REE contents (ΣREE) increased from the pre-storm sample (ΣREE = 261.5 ppt; blue square in Fig. 2) to the onset of the hydrograph recession limb (ΣREE = 569.3 ppt; red square), then it decreased to a value lower than the pre-storm sample (ΣREE = 184.4 ppt; green square).

During the 2016 event, the *Mora* river discharge showed a secondary peak an hour after the highest hourly rainfall (2016/11/24 9:00 AM) and reached its maximum peak flow 14 h later (2016/11/24 11:00 PM, Fig. 3). The discharge returned to low-flow value (250 l/s)

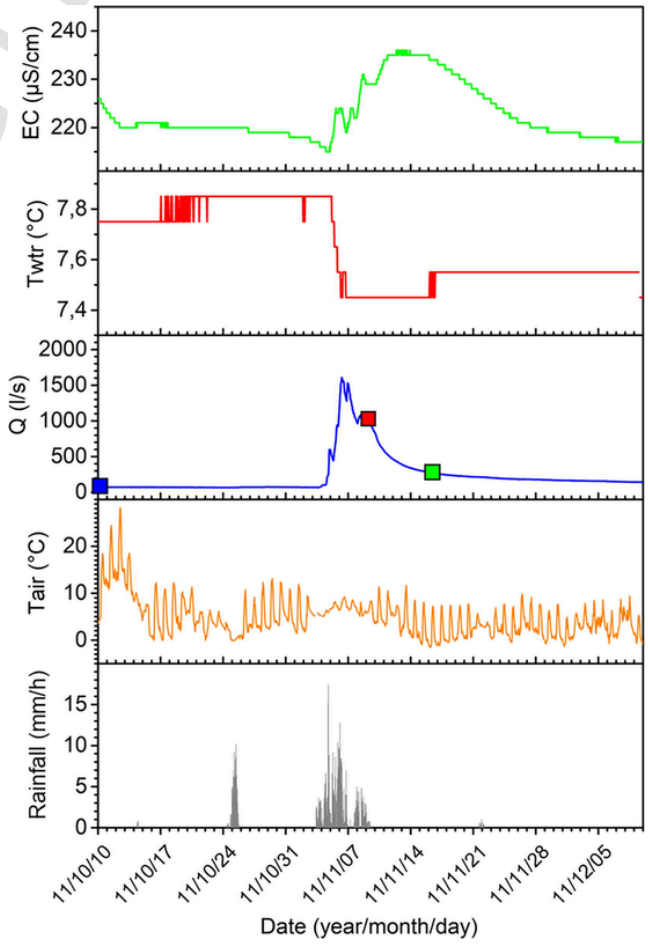

Fig. 2. *Mora* river hydrograph and chemographs (T, EC) during November 2011 monitoring. The water samplings are highlighted by the colored squares. Rainfall and air temperature at the *Borello* meteorological station are also reported.

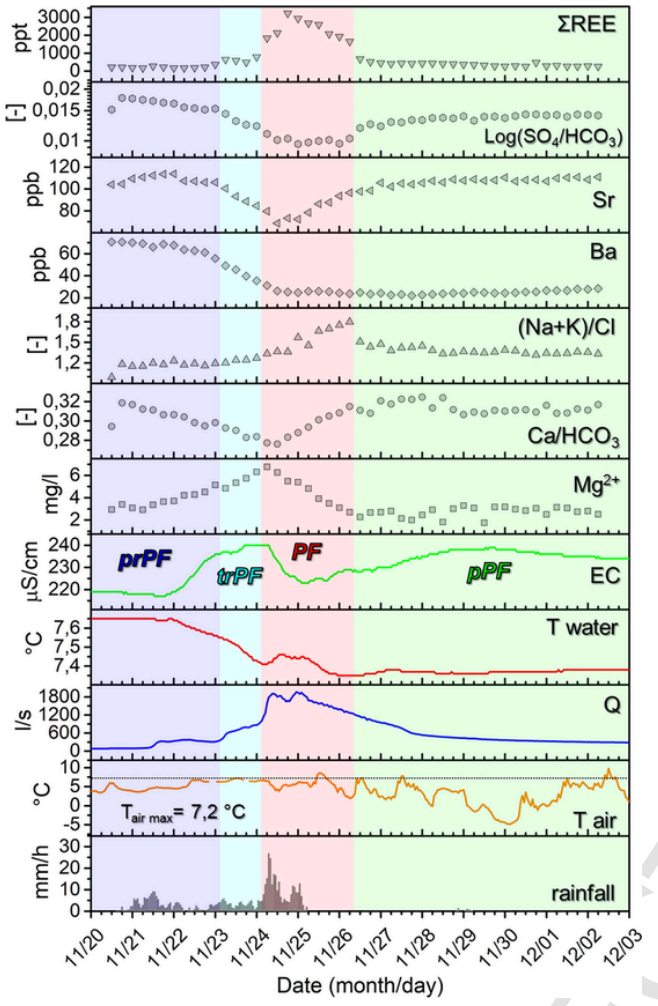

Fig. 3. Meteorological time series (precipitation and air T), TM hydrograph, and chemographs for the November 2016 flood. The colors represent four different groups of normalized REE spider diagrams (blue = pre-peak flow (prPF), cyan = transition to peak flow (trPF), red = peak flow (PF) and green = post peak flow (pPF), see below). Maximum air temperature during the storm is highlighted.

a week after peak flow. Water temperature decreased as flow started to increase. It reached its minimum in the middle of the recession limb, then started to slowly increase and returned to pre-flood values at the beginning of February 2017. EC first increased sharply, reaching its maximum 16 h before the first flood peak, then it showed a negative low synchronous with the maximum flood peak. It slowly increased again during the recession limb reaching almost the same value recorded during the rising limb. Then it slowly decreased and returned to pre-flood values at the end of December 2016. Strontium, calcium to bicarbonate, and the logarithm of the sulfate to carbonate ratios decreased from the beginning of the storm to the first flood peak. They returned to pre-flood values after the flood peak. Magnesium, total REE content (ΣREE), and the alkali to chloride ratio increased during the flood peak. In particular, the Mg trend mirrored the Ca/HCO_3 one whereas the highest ΣREE (3221.6 ppt) was reached 12 h later. The alkali to chloride ratio was maximum 36 h after the maximum ΣREE. Barium content decreased slowly during the flood and did not return to pre-flood values. Aluminum, Iron, and Manganese showed a good correlation with the ΣREE trend (R^2 = 0.95; see the Supplementary Material for Al, Fe and Mn chemographs).

The chemical analyses revealed that the *Mora* river water samples are, overall, of the bicarbonate-calcic type during both storm events (Fig. 4). The magnesium, alkali, and chloride ions have the highest

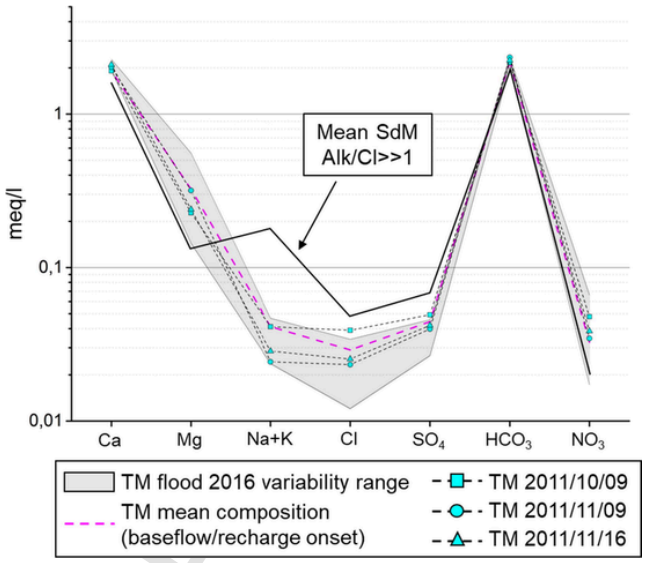

Fig. 4. Schoeller diagram of *Mora* river hydrochemical composition during the 2011 and 2016 flood events. The black line represents the *Sorgente dei Matti* mean composition (SdM).

variability in composition. The *Sorgente dei Matti* spring has a bicarbonate-calcic signature and a high alkali to chloride ratio (mean value 6.63). The summary statistic of trace elements (Al, Mn, Fe, Rb, Sr and Ba), and lanthanides (ΣREE) during the two floods can be found in the Supplementary Material.

The pre-storm (2011) sample showed a normalized REE pattern with a positive Eu_n anomaly and a rising trend in Heavy Rare Earth Elements ($HREE_n$). The during-storm sample was characterized by the absence of the Eu_n positive anomaly and a slightly decreasing trend in $HREE_n$. The post-storm sample showed a Eu_n positive anomaly and a $HREE_n$ trend like that of the previous sample (Fig. 5). Based upon the shape of the 2016 event REEs patterns and sampling times (samples chronologically ordered), four different pattern groups can be distinguished (Fig. 5): Group one (pre-peak flow, prPF) that includes samples 1 to 11 (mid 2016/11/20 to the beginning of 11/23) with a Eu_n

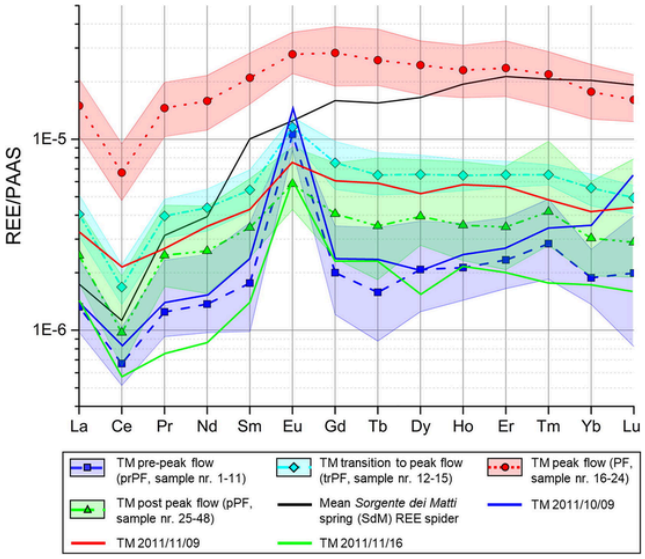

Fig. 5. Spider diagram of REEs concentrations normalized to PAAS. The patterns of the samples collected during the 2016 flood are grouped according to their shape and time position. The variability range (and the mean value, lines + points pattern) of each group is plotted instead of individual sample patterns for clarity. The *Sorgente dei Matti* (SdM) mean REE pattern is reported for comparison (black line).

positive anomaly and rising $HREE_n$ trend. Group two (transition to peak flow, trPF) comprising samples 12 to 15 (11/23 to the beginning of 11/24) with a small Eu_n positive anomaly and an inversion of the $HREE_n$ trend.

Group three (peak flow, PF; samples 16 to 24, from 11/24 early morning to 11/26 early morning) with no Eu_n anomaly and a $HREE_n$ trend similar to that observed in group two. The highest ΣREE content (ΣREE = 3221.6 ppt for sample 18) is in this group. Group four (post-peak phase, pPF; samples 25 to 48) with a small positive Eu_n anomaly.

4.2. Hydrological and hydrochemical monitoring of secondary tributaries

The summary statistics of the hydrological and physico-chemical parameters of the inflows monitored during the two storms are reported in Table 3. Mean values for each inflow are also reported for comparison. The average values were calculated from data collected in the last 10 years.

Table 3
Statistics of discharge Q, water temperature T, and electrical conductivity EC of the inflows monitored during the two storms.

	Milano (M)			*Polletta (PTTA)*		
	Q	T	EC	Q	T	EC
	l/s	°C	µS/cm	l/s	°C	µS/cm
mean						
Mean	0.04	9.55	411.1	0.01	9.46	338.5
Median	0.005	9.33	411.0	$<10^{-4}$	9.35	339.0
Min	0.00	9.10	286.8	0.00	9.09	215.0
Max	0.54	10.60	536.0	0.33	10.65	456.0
2011						
Mean	0.003	9.43	391.9	0.02	9.45	–
Range	0.16	1.30	101.0	0.33	1.50	–
Min	0.00	9.10	321.0	0.00	9.15	–
Flood peak	0.16	10.40	422.0	0.33	10.65	–
2016						
Mean	0.09	9.66	405.3	0.01	9.49	334.1
Range	0.54	1.40	127.0	0.13	0.79	133.0
Min	0.0003	9.20	345.0	0.00	9.22	266.0
Flood peak	0.54	10.60	472.0	0.13	10.01	399.0

Milano and *Polletta* have quite constant discharges that decrease to zero only in case of dry summers. The two inflows showed a specific variability for Q, T, and EC (Table 3). The *Milano* drip (M, Fig. 6) reached its highest Q and T during the November 2016 storm. The parameters monitored had a lower variability during the 2011 storm with respect to the 2016 one (Table 3). There was a lag time between rainfall pulses and peak Q, varying from an hour to 11 h for the 2011 event and 2 to 5 h for the 2016 storm.

The *Polletta* (PTTA, Fig. 6) inflow showed a broader parameter variability during the 2011 event than during the 2016 one (Table 3). In November 2011, *Polletta* reached the maximum Q ever recorded and its highest T. The lag time between rainfall pulses and the corresponding Q peak is between 2 and 6 h for the 2011 storm whereas it is about 2 weeks for the 2016 one. No EC data were available for the 2011 event, so information about PTTA mineralization was gained from the total dissolved solids (TDS) measured in two samples (Fig. 6a). TDS was higher during the peak flow (307.3 mg/l) than during the recession phase (273.6 mg/l).

Both inflows have a bicarbonate-calcic-magnesian hydrochemical composition that, overall, showed no significant variations during the two storms with respect to their mean composition (see Supplementary Material). The alkali to chloride ratio is almost always close to 1 in both inflows.

The most abundant trace elements and lanthanide concentrations are reported in the Supplementary material. In the *Milano* inflow, ΣREE decreased from the beginning (ΣREE = 179.5 ppt) to the end (ΣREE = 48.0 ppt) of the 2011 event samplings, whereas it increased from the first to the second collected sample in *Polletta* (63.4 ppt and 110.5 ppt, respectively). The REE patterns of the studied inflows are divided in three types: (1) patterns showing a positive $HREE_n$ trend (M 2011/10/09, Fig. 7a), (2) flat pattern (M 2016/11/23, Fig. 7b), and (3) pattern with a negative Ce_n anomaly and a positive Eu_n anomaly (Fig. 7c, d).

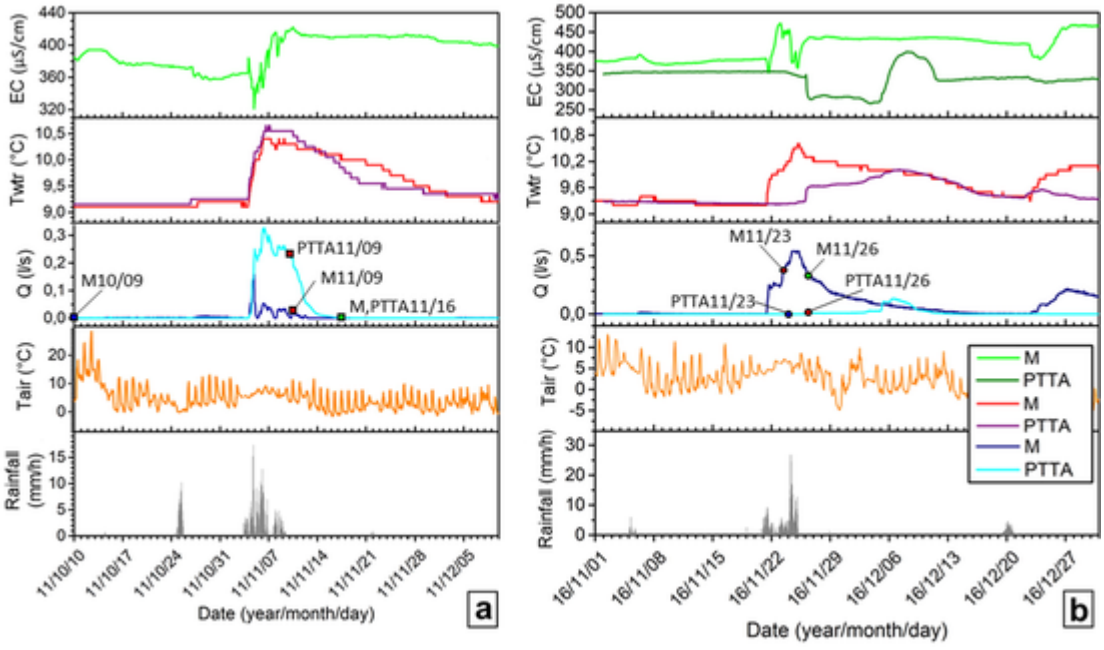

Fig. 6. Hydrographs and chemographs of *Milano* and *Polletta* during the November 2011 (a) and November 2016 storms (b). Water samplings (labelled as "site code month/day") are represented by the colored squares and circles.

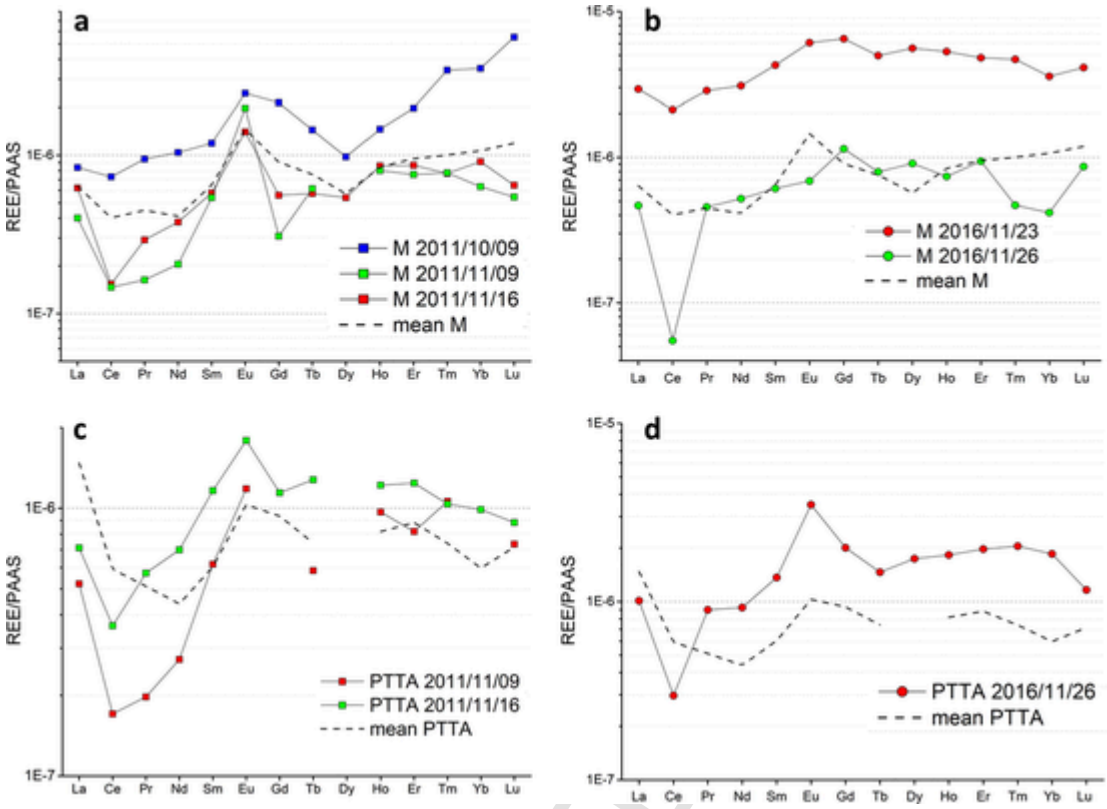

Fig. 7. Normalized REE patterns of the two inflows. (a) *Milano* (M) and *Polletta* (PTTA) inflows during the two storms. Mean REE patterns are reported for comparison (source: *Bossea* karst laboratory).

5. Discussion

5.1. Mora river behavior during the 2016 flood: recognition of the different water sources

The *Mora* river showed a complex behavior during the extreme flood occurred in November 2016. This complexity can be related to different contributions of the underground catchment compartments to flood flow. As mentioned in Section 2.1, the *Bossea* karst system has a complex architecture where several lithologies concur to the storage of water. All parameters monitored during the flood suggest a piston-flow behavior, so that the storm pulse transmits water already stored in the underground drainage system.

The peculiar characteristic of the water stored in *L-Kc* is the high alkali to chloride ratio and the shape of the REE pattern, as shown in the *Sorgente dei Matti* spring (Fiorucci et al., 2015). The contribution of non-carbonate lithologies can be assessed by comparing the major chemistry with trace elements data (chemographs and spider diagrams) and hydrological parameters. Hence, four flow phases corresponding to the four REEs pattern groups can be distinguished (Fig. 3):

1. Pre-Peak Flow phase (prPF): during this stage, the discharged water was mainly from the calcium carbonate rocks, with minor inflows from the shales as suggested by the mean REE pattern and by the sulfate to bicarbonate ratio chemograph.
2. Transition to Peak Flow phase (trPF): the sustained precipitations led to a marked increase of discharge; the discharged water had a more magnesium-calcic signature due to carbonate dissolution.
3. Peak Flow phase (PF): this stage includes the peak discharge and the following initial part of the recession limb. The most important contribution from the non-carbonate lithologies happened during this phase, as suggested by the alkali to chloride ratio, EC graphs, and REE patterns. The low EC is related to drainage of a large portion of the underground catchment rather than to neo-infiltration water, as suggested by the small T peak. The low water mineralization during this phase is related to the lithology of the drained area. An early major contribution came from the quartzite drainage system, as suggested by the ΣREE, Fe, Al, and Mn trends. Then, the meta-volcanic component overshadowed the quartzite one as highlighted by the simultaneous decrease of ΣREE and increase of the alkali to chloride ratio.
4. Post-Peak Flow Phase (pPF): in this phase the underground system recovers from the flood perturbation. The increasing mineralization, the chemographs, and the REE patterns suggest that this portion of the hydrograph is mostly fed by calcium-carbonate portion of the catchment and secondarily by the metavolcanic portion of the catchment (the alkali/chloride ratio decreased but not to pre-flood values) whereas the shale contribution does not seem relevant ($HREE_n$ trend inversion and SO_4/HCO_3 ratio lower than pre-flood levels). Considering the EC trend, the interval of recovery to pre-flood values is about a month.

The hydrodynamics and hydrochemical behavior of the *Mora* river during the 2016 flood appears complex and showed some uncommon features if compared to normal infiltration events or to storms having lower magnitude than the 2016 event, such as the one discussed in the following sub-section.

5.2. Mora river 2011 flood

The monitoring of the November 2011 rainfall event shows that strong (not extreme for the area) precipitations homogeneously distributed over a long-time interval trigger an impulsive response of the karst system, which is spatially limited with contributions confined to

the carbonate reservoir (Fig. 8). The low-flow phase preceding the storm pulse was characterized by a prevalent contribution of the calcium carbonate host rock, with minor inputs from the drainage network developed in the shales (see the REE spider diagram in Fig. 8). The principal flood discharge phase (rising limb, peak flow, and recession onset) is characterized by a general increase in mineralization but with some small relative lows. The sample collected during the last EC relative low has a REEs pattern that can be correlated to the *L-Kc* signature, although the alkali to chloride ratio is about one.

This discrepancy with the behavior observed during the November 2016 flood can be explained with a less important contribution from the *L-Kc*, which is enough to perturb the chemical signal but not as much as during the 2016 event. The comparison of ΣREE content in the peak flow phases of 2011 and 2016 highlights the different magnitude of the non-carbonate portions of the catchment during the two infiltration events (569.3 against 3221.6 ppt).

5.3. Comparison between floods

As pointed out by Civita et al. (2005), the *Bossea* karst system cannot drain the whole amount of precipitation that falls during time-sustained extreme storm events such as the November 2016 one when one third of the 2016 total rainfall was concentrated in the five days of the storm. The external morphology of the karst system, characterized by steep slopes of marble outcrops bordered by low-permeable rocks, limits the infiltration of water from both surface stream runoff (developed mostly along the tectonic contact between permeable and low-permeable rocks) and direct recharge from surface infiltration. Despite being piston-flow the mechanism observed during both floods, the different magnitude of the two meteorological events led to the drainage of different portions of the karst system. During the November 2011 storm, water was drained mostly from the marbles of the *H-Kc* in the area proximal to the *Bossea* cave (Fig. 9a). The flood involved progressively larger sectors of the karst system but the contribution of the *L-Kc* was limited and occurred only during the peak flow phase (PF, red dot-

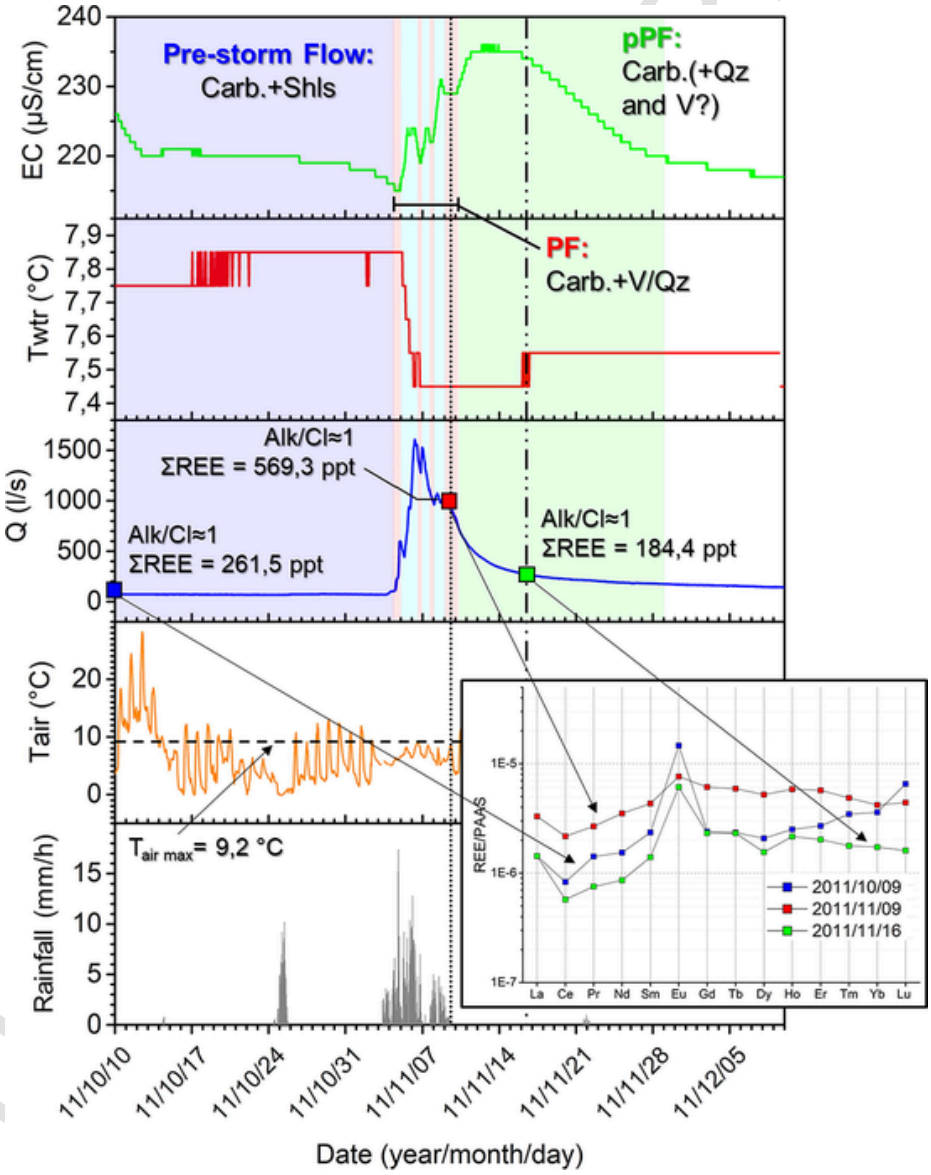

Fig. 8. TM hydrograph and chemographs during the November 2011 storm event. The box reports the spider diagrams of the samples collected 3 weeks before (blue rectangles), 4 days after (red rectangles) and 9 days after (green rectangles) the storm event. The labels "Carb.", "Shls", "V" and "Qz" stand for carbonate, shales, metavolcanics, and quartzites, respectively.

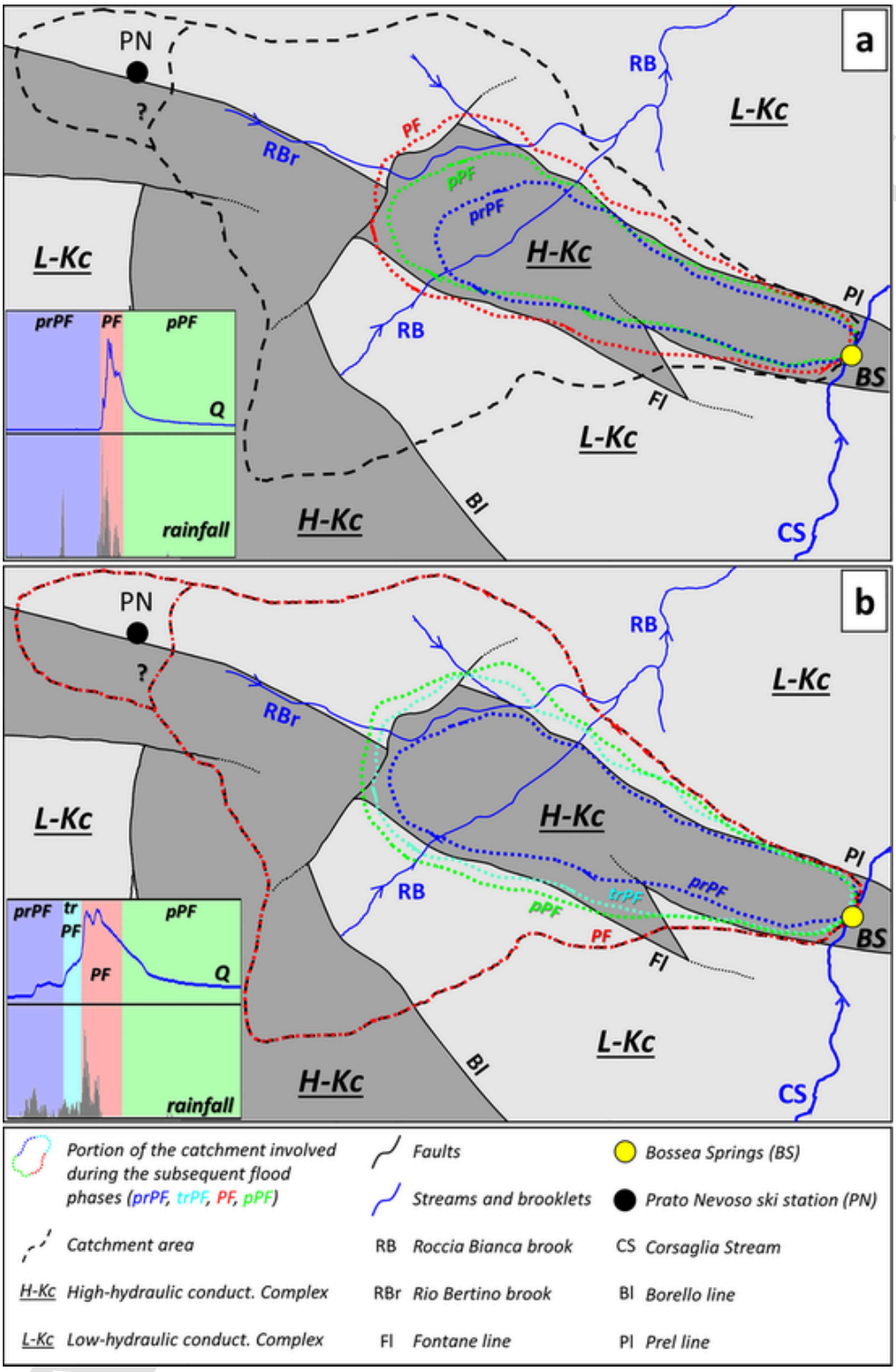

Fig. 9. Comparison of *Mora* river floods. (a) November 2011 and (b) November 2016 events. The blue, cyan, red and green dotted lines represent the drainage area involved during the pre-peak flow (prPF), transition to peak flow (trPF, recognized only for the 2016 event), peak flow (PF) and post-peak flow (pPF) phases, respectively. The boxes in the bottom left part of (a) and (b) report the *Mora* river hydrograph during the two events. l-Kc and H-Kc stand for *Low-hydraulic conductivity Complex* and *High-hydraulic conductivity Complex*, respectively.

ted line, Fig. 9a). The extreme precipitations of the 2016 event caused the activation of the whole catchment during the peak flow phase (PF, red dotted line in Fig. 9b); the non-carbonate inputs occurred also in the transition to peak flow phase (trPF, cyan dotted line, Fig. 9b) and in the whole recession phase (pPF, green dotted line, Fig. 9b).

5.4. The unsaturated zone response to strong precipitation events

The comparison between the water T and EC chemographs and air T (indicator of rainfall T) reveals that the water discharged by the *Milano* drip site during both events was relatively old and was flushed

down by a pressure wave propagation (piston-flow). The characteristics of the two precipitation events, however, led to different timing of activation for each fracture network draining the *Milano* drip site. The alkali to chloride ratio higher than one (1.42) and the positive $HREE_n$ trend (Fig. 7a) could be indicative of contributions from the shale host rock before the 2011 storm onset (pre-piston flow phase, prFl, Fig. 10a). Based on the observed EC trends, two sub-phases of piston flow were distinguished during both events: a carbonate (PsFl C-d) and a non-carbonate dominated (PsFl nC-d, Fig. 10) ones. The timing of the non-carbonate sub-phase is related to the highest discharge pulses during both events: in November 2011, the maximum discharge is reached during the first pulse of the storm whereas the peak flow of 2016 was reached in the late phase of the rainfall event. The inputs from the non-carbonate rocks were intermittent during both storms. The possibility that water from the *L-Kc* could feed this drip site was confirmed also by some tracer tests performed in 2007 (Banzato et al., 2013). After peak flow, the drip is fed mainly by the Ca-Mg-carbonates, as shown by the EC trends during both storms (recovery phase, "Rec. Crbn" in Fig. 10) and the hydrochemical analyses (REE spider diagram in Fig. 7a, Supplementary Material).

Polletta showed an impulsive, piston-flow behavior during both storm events (Fig. 11) with different characteristics of the monitored parameters. TDS, alkali/chloride ratio, and the REE spider diagram suggest water drainage from the carbonate rocks overlying the detachment surface (Fig. 1c, d) during the second half of the storm peak and in the post-storm phase (Fig. 11). *Polletta* usually shows impulsive response to precipitations during the fall recharge. Its water mineralization indicates a major contribution from the *L-Kc* (relative EC minima) followed by a variable input from the marbles of the *H-Kc* (positive EC peaks). Differently from *Milano*, *Polletta* responded sharply to the precipitation of the 2011 event, showing a single discharge peak. *Milano*, on the contrary, had an intermittent impulsive response to each individual precipitation pulse of the 2011 event. The two weeks' lag precipitation-flow peak shown by *Polletta* during the 2016 storm (Fig. 11b) is unusual during fall recharge. Water T and EC together showed a prolonged piston-flow episode that is characterized by two sub-phases. There was first a well-defined input of less mineralized water from the *L-Kc* (non-carbonate piston flow, nC-PsFl, Fig. 11b), followed by a sharp increase of EC marking the transition to a pure carbonate contribution (C-PsFl). It is still unclear which mechanism triggers this behavior in the fall season, but it is likely related to the amount of water stored in the small fractured aquifer that feeds the *Polletta* spring inflow (see Section 5.4.1 for more details).

5.4.1. Unsaturated zone architecture and its response to extreme precipitation

Overall, the unsaturated zone of the two inflows showed a piston-flow behavior during both storm events but, due to their structural position, there were differences in timing and in drainage system involved (Fig. 12).

The behavior of *Polletta* depends upon the balance between water stored in its reservoir, water percolating from the unsaturated zone, and intensity of the meteorological event. Its perched reservoir developed primarily in the fractures of the upper damage zone of the detachment (bottom part of the marble sequence) and secondarily in the bottom part of the damage zone (topmost part of the metavolcanics). Here, we refer to damage zone as the volume of deformed wall rock around a fault surface that results from the initiation, propagation, interaction and build-up of fractures along faults (Kim et al., 2004). *Polletta* hydrology and hydrochemistry are, therefore, controlled by the fractured rock volume drained in the vicinity of the detachment and in the unsaturated zone above. The intensity of precipitation controls the efficient transmission of the pressure wave first in the unsaturated zone and then in the perched reservoir. During piston flow, the *Polletta* spring inflow drains first the non-carbonate water in the small aquifer (stage 2 "nC Piston flow" in Fig. 12a) and later the water percolating from the

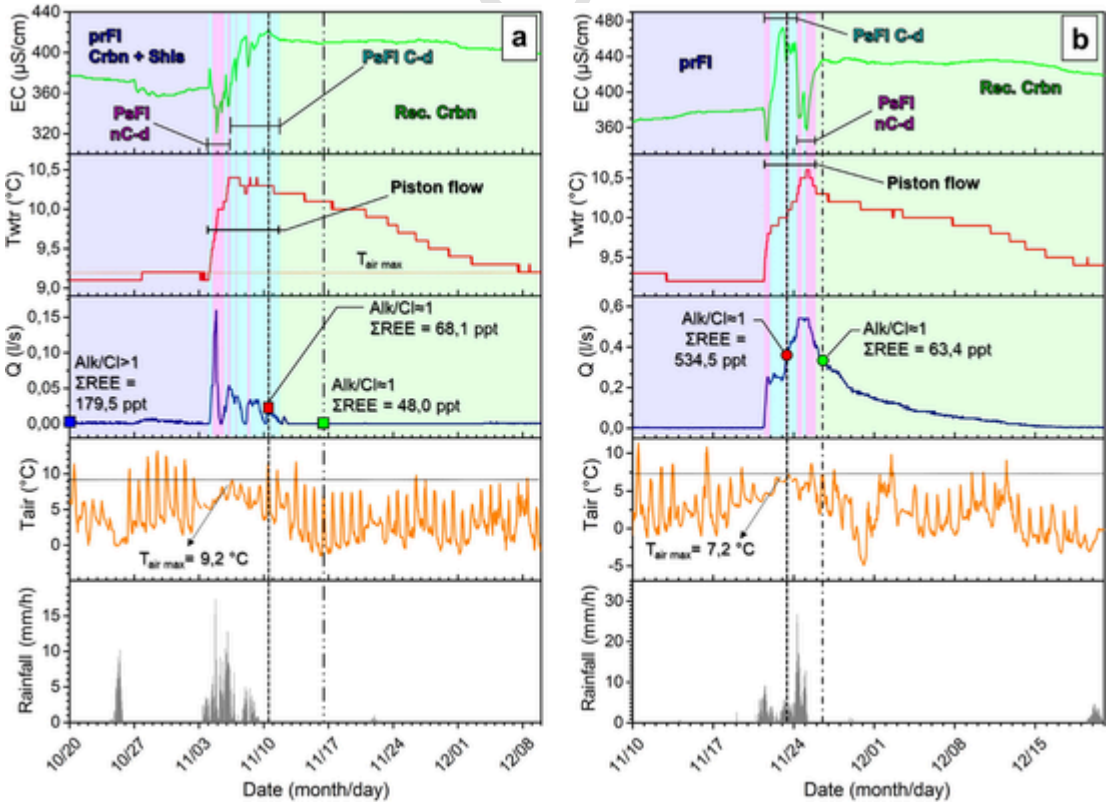

Fig. 10. *Milano* drip hydrograph, and chemographs during the 2011 (a) and 2016 storms (b). Colored squares and circles indicate analyzed samples.

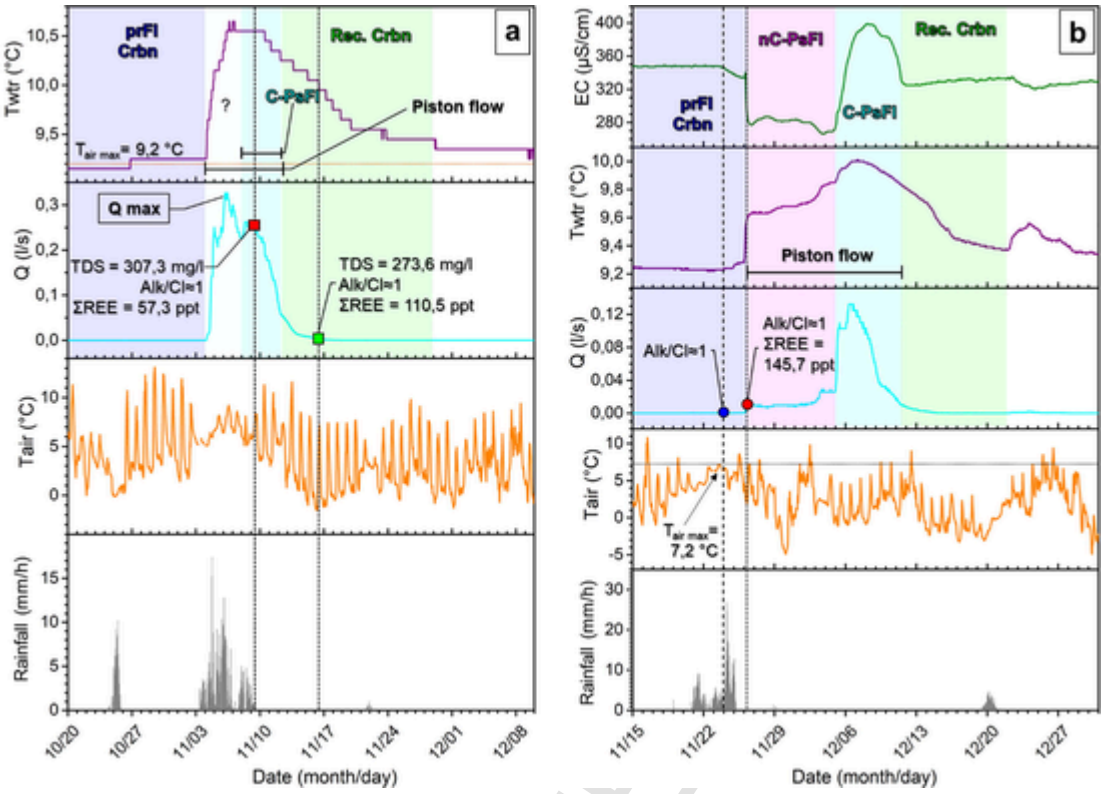

Fig. 11. *Polletta* hydrographs, chemographs, and REE spider diagrams during the 2011 (a) and 2016 (b) storms. Colored squares and circles indicate analyzed samples.

unsaturated zone (stage 3 "C PF" in Fig. 12a). Its discharge, therefore, is the result of a piston flow masked by the presence of the small aquifer in the upper damage zone of the detachment where water acquires the chemical signature characteristic of the host rock. Probably, the low permeability of the *Polletta* reservoir delays the transmission of hydraulic pressure from the unsaturated zone, resulting in the lag between peak precipitation and peak discharge observed during the 2016 event.

The functioning of the *Milano* drip site depends primarily on the architecture of its feeding systems (i.e. fracture network permeability and organization) and secondarily on the characteristics of the meteorological events. *Milano* represents the most typical and efficient flow system in the *Bossea* unsaturated zone, namely discharge through karstified bedding junctions (Antonellini et al., 2019). During the two storm events, *Milano* showed that non-carbonate inputs are most important during peak discharge (stage 3 "nCd-Fl" in Fig. 12b) when the whole drip drainage system is activated. The magnitude of the precipitation combined with the initial saturation conditions inside the fractures determined the amount of old water discharged.

6. Conclusions

The presence of an underground karstological laboratory, makes the *Bossea* show cave a unique test site for the hydrological investigation of flood events, as shown in this study. The well-equipped monitoring infrastructure of the *Bossea* cave permitted to assess the karst system response during the November 2011 and November 2016 meteorological and flooding events. For the first time, it was possible to study at the same time the hydrochemical and hydrological evolution during extreme storms with different magnitudes of an underground river and drip sites.

Overall, *Bossea* had a piston-flow response to the 2016 extreme infiltration, like the behavior shown during antecedent floods. This behavior is strictly related to the structural and morphological setting of the karst system.

The *Mora* river showed a progressive increasing contribution to flow from the non-carbonate compartments during the peak of both floods, highlighting the involvement of broader sectors of the catchment. However, the involvement of the non-carbonate sectors is strongly dependent on the duration and the intensity of the meteorological event, because infiltration needs to be efficient across most of the catchment for the non-carbonate inputs to be relevant. This is evident from the comparison between the 2011 and 2016 floods: the former event was significantly weaker than the latter one, so that infiltration was reduced and the propagation of hydraulic pressure was efficient only in the proximal area of the catchment in contrast to what happened during the 2016 flood.

The response of each individual portion of the unsaturated zone is strongly influenced by its saturation conditions that are, in turn, dependent on the fracture network architecture. The inflows' chemical signatures and their temporal variability confirm the heterogeneity of the unsaturated zone of this system and its relevance on their discharge during infiltration events of variable magnitude.

The monitoring of *Bossea* confirmed the necessity to investigate several parameters to unravel the functioning of a "multi-reservoir" complex karst system. The piston-flow behavior of both the main underground river and the unsaturated inflows was recognized only by integrating hydrological, continuous, and discrete hydrochemical data. This study confirms that the unsaturated zone cannot be simply considered a water transfer pathway to the saturated zone of karst aquifers but a proper, although heterogeneous, storage compartment. The local structural setting can further enhance its complexity, but its functioning can be unraveled coupling the detailed knowledge of the geological setting and the careful interpretation of the aforementioned data. The methodology that we used here to identify the contributions of different sectors of the karst system to underground flow can also be applied to other fractured aquifers characterized by strong geological heterogeneities such as the Alpine-type karst systems. As stated in the intro-

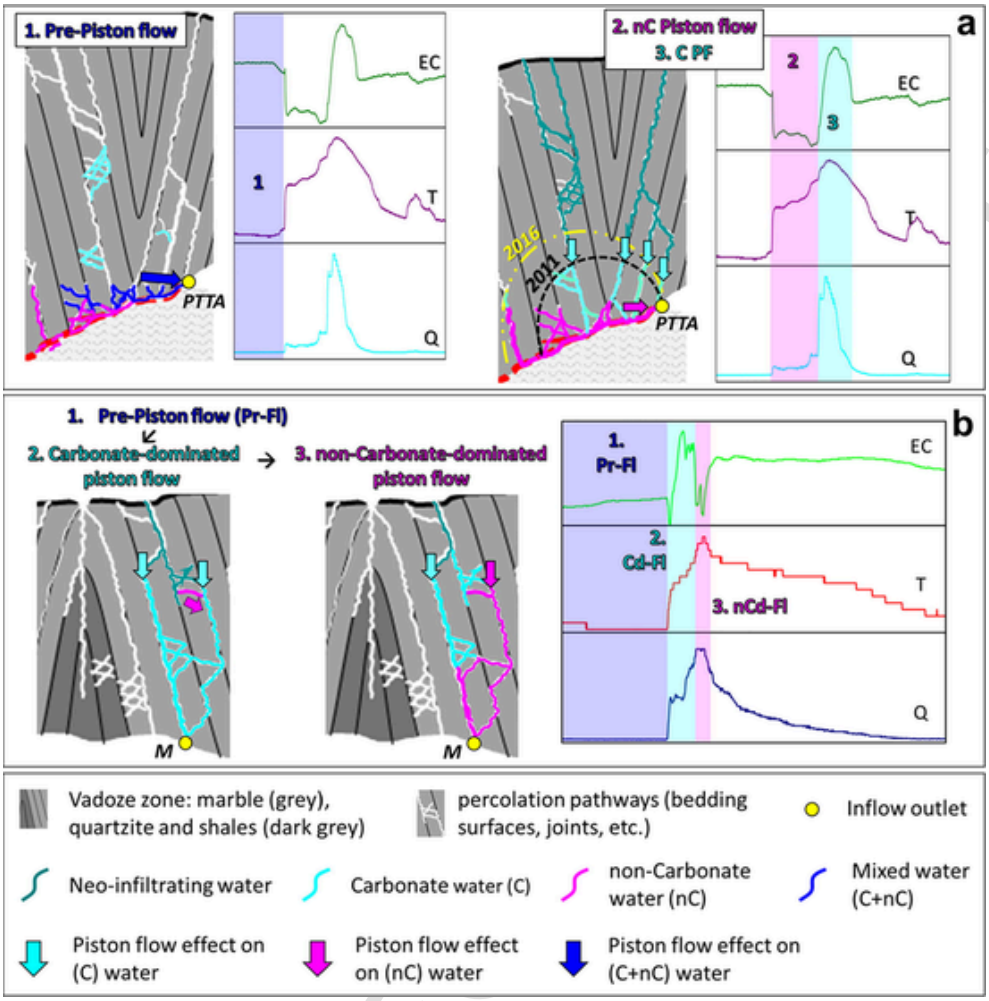

Fig. 12. Model for water circulation in the unsaturated zone of the *Bossea* karst system. See the red rectangles in Fig. 1c, d for the position of the inflows described in each box. *Polletta* spring inflow (PTTA) showed piston flow phenomena masked by the drainage of its perched reservoir. The water stored in its perched aquifer is a mixture of carbonate water (C) from the unsaturated zone, and a non-carbonate water (nC) stored in the metavolcanics of the lower damage zone. *Milano* (M) drip site is representative of flow along karstified bedding junctions, and it shows evidence of episodic non-carbonate water inputs.

duction, this karst type can be found wherever carbonate rocks are involved in orogenetic processes (Alps, Rocky Mountains, Caledonides, etc.). In such contexts, the use of multiple parameters is critical to recognize the contribution of allogenic and autogenic recharge, the challenge being the identification of the parameters that are most sensitive (i.e. more representative) to flood perturbation and recharge area properties. REE normalized patterns and chemograph analysis of REE and trace elements concentrations, major ions' ratios (alkali to chloride and secondarily sulfate to bicarbonate), and water physico-chemical parameters (EC and T) were demonstrated to be powerful tools to discriminate carbonate from non-carbonate (volcanoclastic and siliciclastic) contributions to flow. Despite being relatively widespread, the hydrodynamics of the often complex Alpine-type karst aquifers is still poorly known. Our study showed that only long-term and well-integrated monitoring and sampling can help unravel the behavior of such karst systems, particularly for defining the proper monitoring strategy to study the consequences of extreme meteorological events on these aquifers. The ongoing hydrological and hydrochemical monitoring carried out by the *Bossea* underground laboratory may allow to investigate the hydrodynamic response of the aquifer to other future anomalous storm events under different hydrologic conditions (e.g. spring snowmelt).

Uncited references

.

CRediT authorship contribution statement

Alessia Nannoni: Visualization, Methodology, Investigation, Data curation, Writing - original draft, Visualization. **Bartolomeo Vigna:** Visualization, Investigation, Resources, Writing - review & editing. **Adriano Fiorucci:** Validation, Formal analysis, Data curation, Writing - review & editing. **Marco Antonellini:** Writing - review & editing, Supervision. **Jo De Waele:** Writing - review & editing, Supervision, Project administration.

Declaration of Competing Interest

The authors declare that they have no known competing financial interests or personal relationships that could have appeared to influence the work reported in this paper.

Acknowledgements

The hydrochemical and hydrological data belong to the Karst Hydrology Laboratory of the Department of Land and Infrastructure Engineering (DIATI) – Polytechnic of Turin, director Prof. Bartolomeo Vi-

gna. The Authors thank the reviewers for their suggestions which helped to improve the manuscript.

Appendix A. Supplementary data

Supplementary data to this article can be found online at https://doi.org/10.1016/j.jhydrol.2020.125493.

References

Antonellini, M., Nannoni, A., Vigna, B., De Waele, J., 2019. Structural control on karst water circulation and speleogenesis in a lithological contact zone: the Bossea cave system (Western Alps, Italy). Geomorphology 345. doi:10.1016/j.geomorph.2019.07.019.

ARPA Piemonte, 2011. Evento meteoidrologico del 4-8 novembre 2011. Arpa Piemonte, Torino.

ARPA Piemonte, Regione Piemonte, 2018. Gli eventi alluvionali in Piemonte – Evento del 21–25 novembre 2016. Arpa Piemonte, Torino.

Audra, P., Bini, A., Gabrovšek, F., Häuselmann, P., Hobléa, F., Jeannin, P., Kunaver, J., Monbaron, M., Šušteršič, F., Tognini, P., Trimmel, H., Wildberger, A., 2007. Cave and karst evolution in the Alps and their relation to paleoclimate and paleotopography. Acta Carsologica 36, 53–67.

Baedke, S.J., Krothe, N.C., 2001. Derivation of effective hydraulic parameters of a karst aquifer from discharge hydrograph analysis. Water Resour. Res. 37, 13–19. doi:10.1029/2000WR900247.

Baldini, J.U.L., McDermott, F., Baldini, L.M., Ottley, C.J., Linge, K.L., Clipson, N., Jarvis, K.E., 2012. Identifying short-term and seasonal trends in cave drip water trace element concentrations based on a daily-scale automatically collected drip water dataset. Chem. Geol. 330–331, 1–16. doi:10.1016/j.chemgeo.2012.08.009.

Banzato, C., Marchionatti, F., Vigna, B., 2013. Drainage index calculated with artificial tracers. AQUA Mundi 67–75. doi:10.4409/Am-059-13-0053.

Banzato, C., De Waele, J., Fiorucci, A., Vigna, B., 2011. Study of springs and karst aquifers by monitoring and geochemical analysis, in: H2Karst, 9th Conference on limestone hydrogeology, Besançon, France, September 1-3, 2011. pp. 45–48.

Berglund, J.L., Toran, L., Herman, E.K., 2019. Deducing flow path mixing by storm-induced bulk chemistry and REE variations in two karst springs: with trends like these who needs anomalies? J. Hydrol. 571, 349–364. doi:10.1016/j.jhydrol.2019.01.050.

Civita, M., Gandolfo, M., Peano, G., Vigna, B., 2005. The recharge-discharge process in Bossea cave underground basin (NW Italy). In: Maraga, F., Arattano, M. (Eds.), Progress in Surface and Subsurface Water Studies at Plot and Small Basin Scale, Turin, Italy, 13–17 October 2004. International Hydrological Programme, Paris, pp. 145–151.

Civita, M., Vigna, B., 1985. Analysis of Bossea Cave Hydrogeological System (Maritime Alps, Italy). In: Proceedings of the Ankara-Antalya Symposium. pp. 101–114.

De la Torre, B., Mudarra, M., Andreo, B., 2020. Investigating karst aquifers in tectonically complex alpine areas coupling geological and hydrogeological methods. J. Hydrol. X 6, 100047. doi:10.1016/j.hydroa.2019.100047.

Desmarais, K., Rojstaczer, S., 2002. Inferring source waters from measurements of carbonate spring response to storms. J. Hydrol. 260, 118–134. doi:10.1016/S0022-1694(01)00607-2.

Doctor, D.H., Alexander, E.C., Petrič, M., Kogovšek, J., Urbanc, J., Lojen, S., Stichler, W., 2006. Quantification of karst aquifer discharge components during storm events through end-member mixing analysis using natural chemistry and stable isotopes as tracers. Hydrogeol. J. 14, 1171–1191. doi:10.1007/s10040-006-0031-6.

Filippini, M., Squarzoni, G., De Waele, J., Fiorucci, A., Vigna, B., Grillo, B., Riva, A., Rossetti, S., Zini, L., Casagrande, G., Stumpp, C., Gargini, A., 2018. Differentiated spring behavior under changing hydrological conditions in an alpine karst aquifer. J. Hydrol. 556, 572–584. doi:10.1016/j.jhydrol.2017.11.040.

Fiorucci, A., Moitre, B., Vigna, B., 2015. Hydrogeochemical study of Bossea karst system, in: Kataev, V.N., Zolotarev, D.R., Shcherbakov, S.V., Shilova, A.V. (Eds.), Proceedings of the International Symposium in Environmental Safety and Construction in Karst Areas. Perm, Russia, 26–29 May 2015. Perm State University, Perm, pp. 290–294.

Gill, L.W., Babechuk, M.G., Kamber, B.S., McCormack, T., Murphy, C., 2018. Use of trace and rare earth elements to quantify autogenic and allogenic inputs within a lowland karst network. Appl. Geochem. 90, 101–114. doi:10.1016/j.apgeochem.2018.01.001.

Grasso, D.A., Jeannin, P.-Y., 2002. A global experimental system approach of karst springs' hydrographs and chemographs. Ground Water 40, 608–618. doi:10.1111/j.1745-6584.2002.tb02547.x.

Hartmann, A., Goldscheider, N., Wagener, T., Lange, J., Weiler, M., 2014. Karst water resources in a changing world: review of hydrological modeling approaches. Rev. Geophys. 52, 218–242. doi:10.1002/2013RG000443.

Jex, C.N., Mariethoz, G., Baker, A., Graham, P., Andersen, M.S., Acworth, I.R., Edwards, N., Azcurra, C., 2012. Spatially dense drip hydrological monitoring and infiltration behaviour at the Wellington Caves, South East Australia. Int. J. Speleol. 41, 283–296. doi:10.5038/1827-806X.41.2.14.

Kim, Y.-S., Peacock, D.C.P., Sanderson, D.J., 2004. Fault damage zones. J. Struct. Geol. 26, 503–517. doi:10.1016/j.jsg.2003.08.002.

Liu, A.W., Brancelj, A., Brenčič, M., 2014. The hydrochemical response of cave drip waters to different rain patterns (a case study from Velika Pasica Cave, central Slovenia). Carpathian J. Earth Environ. Sci. 9, 189–197.

Markowska, M., Baker, A., Treble, P.C., Andersen, M.S., Hankin, S., Jex, C.N., Tadros, C.V., Roach, R., 2015. Unsaturated zone hydrology and cave drip discharge water response: implications for speleothem paleoclimate record variability. J. Hydrol. 529, 662–675. doi:10.1016/j.jhydrol.2014.12.044.

McLennan, S.M., 1989. Rare earth elements in sedimentary rocks: influence of provenance and sedimentary processes. Rev. Mineral. Geochem. 21, 169–200.

Möller, P., Dulski, P., Salameh, E., Geyer, S., 2006. Characterization of the sources of thermal spring- and well water in Jordan by rare earth element and yttrium distribution and stable isotopes of H_2O. Acta Hydrochim. Hydrobiol. 34, 101–116. doi:10.1002/aheh.200500614.

Mudarra, M., Andreo, B., 2011. Relative importance of the saturated and the unsaturated zones in the hydrogeological functioning of karst aquifers: the case of Alta Cadena (Southern Spain). J. Hydrol. 397, 263–280. doi:10.1016/j.jhydrol.2010.12.005.

Peano, G., Vigna, B., Villavecchia, E., 2005. L'evento alluvionale nell'ottobre 1996 nella Grotta di Bossea. In: Gili, R., Peano, G. (Eds.), Atti Del Convegno Nazionale "L'ambiente Carsico e l'uomo". CAI Cuneo, Cuneo, pp. 407–422.

Perrin, J., Jeannin, P.Y., Zwahlen, F., 2003. Implications of the spatial variability of infiltration-water chemistry for the investigation of a karst aquifer: a field study at Milandre test site, Swiss Jura. Hydrogeol. J. 11, 673–686. doi:10.1007/s10040-003-0281-5.

Plan, L., Decker, K., Faber, R., Wagreich, M., Grasemann, B., 2009. Karst morphology and groundwater vulnerability of high alpine karst plateaus. Environ. Geol. 58, 285–297. doi:10.1007/s00254-008-1605-5.

Poulain, A., Rochez, G., Bonniver, I., Hallet, V., 2015. Stalactite drip-water monitoring and tracer tests approach to assess hydrogeologic behavior of karst vadose zone: case study of Han-sur-Lesse (Belgium). Environ. Earth Sci. 74, 7685–7697. doi:10.1007/s12665-015-4696-9.

Poulain, A., Watlet, A., Kaufmann, O., Van Camp, M., Jourde, H., Mazzilli, N., Rochez, G., Deleu, R., Quinif, Y., Hallet, V., 2018. Assessment of groundwater recharge processes through karst vadose zone by cave percolation monitoring. Hydrol. Process. 32, 2069–2083. doi:10.1002/hyp.13138.

Pronk, M., Goldscheider, N., Zopfi, J., Zwahlen, F., 2008. Percolation and particle transport in the unsaturated zone of a karst aquifer. Ground Water 47, 361–369.

Vesper, D.J., White, W.B., 2004. Storm pulse chemographs of saturation index and carbon dioxide pressure: Implications for shifting recharge sources during storm events in the karst aquifer at Fort Campbell, Kentucky/Tennessee, USA. Hydrogeol. J. 12, 135–143. doi:10.1007/s10040-003-0299-8.

Vigna, B., Banzato, C., 2015. The hydrogeology of high-mountain carbonate areas: an example of some Alpine systems in southern Piedmont (Italy). Environ. Earth Sci. 74, 267–280. doi:10.1007/s12665-015-4308-8.

Vigna, B., Doleatto, D., 2008. La circolazione idrica nella zona non satura di Bossea, in: Gili, R., Peano, G. (Eds.), Ambiente Carsico: I Progressi Degli Studi in Italia Sulla Soglia Del XXI Secolo. Bossea, 21–22 Maggio 2005. Stazione Scientifica di Bossea CAI Cuneo, Cuneo, pp. 51–63.

Vigna, B., Fiorucci, A., Nannoni, A., De Waele, J., 2017. Vadose Zone Hydrogeology In The Bossea Cave. Australian Speleological Federation Inc., Sydney, pp. 222–225.

Vigna, B., Peano, G., Villavecchia, E., De Waele, J., 2017b. The Karstological Subterranean Laboratory Of Bossea Cave (N Italy), in: Moore, K., White, S. (Eds.), Proceedings of the 17th International Congress of Speleology, July 22–28, Sydney, NSW Australia. Australian Speleological Federation Inc., Sydney, pp. 447–451.